

## Focusing high energy X-rays with stacked Fresnel zone plates

I. Snigireva<sup>\*1</sup>, A. Snigirev<sup>1</sup>, V. Kohn<sup>2</sup>, V. Yunkin<sup>3</sup>, M. Grigoriev<sup>3</sup>, S. Kuznetsov<sup>3</sup>,  
G. Vaughan<sup>1</sup>, and M. Di Michiel<sup>1</sup>

<sup>1</sup> ESRF, B.P. 220, 38043 Grenoble, France

<sup>2</sup> Russian Research Centre “Kurchatov Institute”, 123182 Moscow, Russia

<sup>3</sup> IMT RAS, 142432 Chernogolovka, Moscow region, Russia

Received 25 September 2006, revised 12 January 2007, accepted 30 March 2007

Published online 1 August 2007

PACS 07.85.Fv, 41.50.+h, 41.60.Ap, 42.25.Bs, 42.40.Kw, 42.40.Lx

Stacking technique was developed in order to increase focusing efficiency of Fresnel zone plates at high energies. Two identical Si chips each of which containing Fresnel zone plates were used for stacking. Alignment of the chips was achieved by on-line observation of the *moiré* pattern from the two zone plates. The formation of *moiré* patterns was studied theoretically and experimentally at different experimental conditions. To provide the desired stability Si-chips with zone plates were bonded together with slow solidification speed epoxy glue. Technique of angular alignment in order to compensate a linear displacement in the process of gluing was proposed. Two sets of stacked FZPs were produced and experimentally tested to focus 15 and 50 keV X-rays. Gain in the efficiency by factor 2.5 was demonstrated at 15 keV. Focal spot of 1.8  $\mu\text{m}$  vertically and 14  $\mu\text{m}$  horizontally with 35% efficiency was measured at 50 keV. Forecast for the stacking of nanofocusing Fresnel zone plates was discussed.

© 2007 WILEY-VCH Verlag GmbH & Co. KGaA, Weinheim

### 1 Introduction

Over the last years, there is a strong demand for focusing of hard X-rays above 20 keV. The high penetration power of high energy X-rays makes them ideal for non-destructive studies of materials and enables *in situ* measurements of the environment-dependent properties. A number of new applications such as surface and interface scattering, high pressure Compton magnetic scattering, and depth strain analysis using powder micro diffraction require a microfocus beam [1, 2]. Efficient focusing of hard X-rays using diffractive optics such as Fresnel zone plates (FZP) is limited by the ability to manufacture diffracting structures with small outermost zone width and the large thicknesses imposed by the weak interaction of X-rays with matter. With increasing photon energy, the required thickness of phase shifting material increases. For example, for efficient focusing 30 keV X-rays with gold FZP the required structure thickness is 6  $\mu\text{m}$  and structure around 20  $\mu\text{m}$  is needed to focus 100 keV X-rays. In order to achieve small period and high aspect ratios inherent in lithography technique, the sputtered-sliced FZP method was proposed in 1982 [3–5]. Sputtered-sliced FZP have exceptionally high aspect ratio suitable for focusing 100 keV X-rays [5], but the small aperture/acceptance strongly limits applicability of these FZPs. To overcome this limitation to produce thicker FZP, one can attempt a multiple zone plate setup [6, 7].

\* Corresponding author: e-mail: snigireva@esrf.fr, Phone: +33 4 76 88 23 60, Fax: +33 4 76 88 25 42

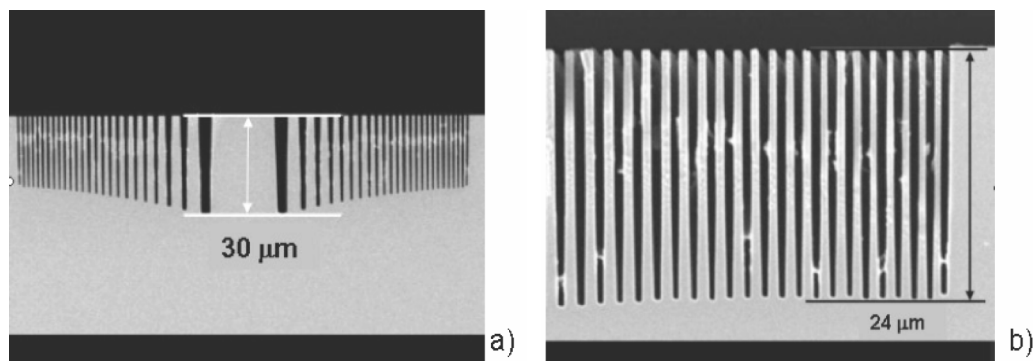


**Fig. 1** SEM images of the FZP cross-section in the central (a) and outer part (b).

We propose to use Si-based FZPs made by modern microfabrication technology, involving lithography and highly anisotropic plasma etching techniques [8]. In addition to a high accuracy and reproducibility, this technique makes possible the realization of number of diffraction elements on-a-chip with a wide range of parameters providing a reasonable energy tunability of microscopy setups at multipurpose synchrotron beamlines. In order for stacked zone plates to behave as one, they have to be positioned laterally and longitudinally within reasonable proximity. Alignment of the two zone plates was done by observing the *moiré* pattern from the two zone plates in real time and maximizing the fringe spacing by moving one of the zone plates. We have developed technique of angular alignment to compensate a linear displacement in the process of gluing. Two types of Si chips were used for stacking to focus 15 and 50 keV X-rays. Stacked sets were experimentally tested and measured focal spot and efficiency are in excellent agreement with calculations that underlines the good quality of the stacked system. Forecast for the stacking of nanofocusing Fresnel zone plates was discussed.

## 2 FZP manufacturing

Silicon based FZPs were manufactured using microfabrication technologies, including the following main processes: electron beam- and photolithography, deep plasma etching and anisotropic wet etching of silicon. Two types of Si chips have been fabricated (see Table 1). The first type of Si-chips contains FZP structures which are 9 μm thick that corresponds to optimum efficiency at the energy around 7.5 keV.

The structures on the Si-chip of second type are 30 μm thick and they are optimized for use at energies around 25 keV. The aspect ratio is more than 50, demonstrating the state-of-the-art of the modern Si microfabrication technology (Fig. 1). Each chip is 18 mm wide and 25 mm height, and all of them are identical. Each chip contains 9 different FZP elements (5-circular and 4-linear) designed as medium and long focal distance optical elements. The main parameters of the FZPs are listed in Table 2. Scanning electron microscope image of FZPs 22 and 32 are shown in Fig. 2.

**Table 1** Si chip parameters.

chip number	membrane thickness*	zone thickness	$E^{**}$	maximum efficiency
chip 1	3 μm	9 μm	6 – 12 keV	30% at 7.5 keV
chip 2	60 μm	30 μm	17 – 40 keV	32% at 23 keV

\* Remaining thickness of Si membrane after etching; \*\*  $E$  is energy range with focusing efficiency > than 20%.

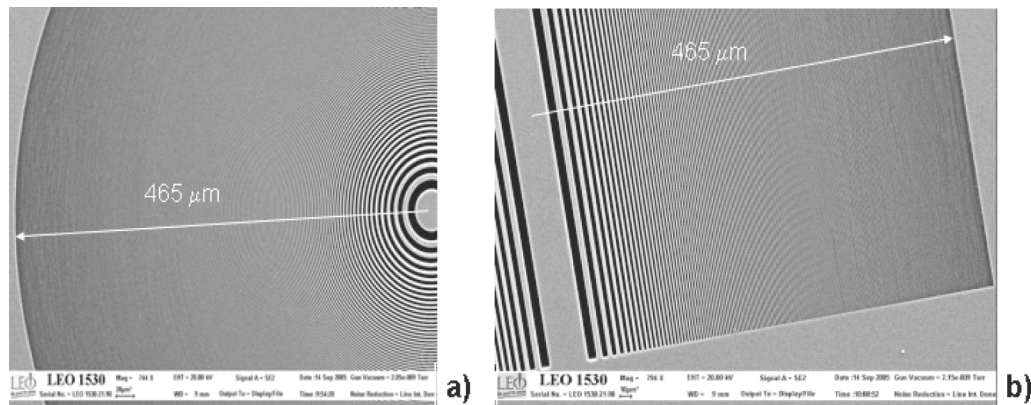


Fig. 2 SEM images of circular FZP 22 and linear FZP 32. Aperture is 930 microns.

### 3 Experiment and discussion

Stacking was performed at the Microoptics test bench (MOTB) located in the 2nd experimental hutch (55 m from the source) of the ESRF BM5 beamline [9]. White radiation from the bending magnet (source size vertically 80  $\mu\text{m}$  and 250  $\mu\text{m}$  horizontally) was collimated by primary and secondary slits and passed through a double crystal monochromator provided an X-ray beam of selected fundamental energy. The FZP chips were mounted on the stages with all necessary angular and linear movements. Two chips with zone plates were joined together in a way that the front side of the first chip is faced to the backside of another one. Therefore, corresponding zone plates are separated from each other by approximately 500 micrometers (substrate thickness). Alignment of the two zone plates is achieved by a straightforward X-ray phase contrast imaging technique by looking at the high resolution CCD camera image of the beam. When you look through one FZP at another, you see a *moiré* pattern, always appears when two repetitive patterns overlap. A slight motion of one of the objects creates large-scale changes in the *moiré* pattern. Increasing the spacing in the *moiré* pattern indicates a correct trend in the alignment and when fringe spacing is infinite the stacking alignment is perfect. The precise and smooth vertical movement of the MOTB table allowed checking alignment of all FZP structures on the chip including linear ones. Alignment was done in the energy range 10–18 keV depending on FZP.

In order for two zone plates to behave as one, they have to be positioned laterally and longitudinally within reasonable proximity. For lateral alignment  $\Delta x$ , a typical requirement is  $\Delta x < 1/3 \Delta r_n$ , where  $\Delta r_n$  is the outermost zone width [10]. We have studied theoretically and experimentally the behavior of the

Table 2 FZP parameters.

FZP number	focal length (cm) $F$ at 8 keV	FZP aperture $A$ ( $\mu\text{m}$ ) and length $L$ ( $\mu\text{m}$ ) for linear	outermost zone width $\Delta r_n$ ( $\mu\text{m}$ )	number of zones, $N$
33 circular	50	$A = 194$	0.4	122
11 linear	100	$A = 387; L = 1000$	0.4	242
12 circular	100	$A = 387$	0.4	242
21 circular	150	$A = 582$	0.4	364
31 linear	150	$A = 582; L = 1000$	0.4	364
13 linear	200	$A = 775; L = 1000$	0.4	484
23 circular	200	$A = 775$	0.4	484
22 linear	240	$A = 930; L = 1000$	0.4	582
32 circular	240	$A = 930$	0.4	582

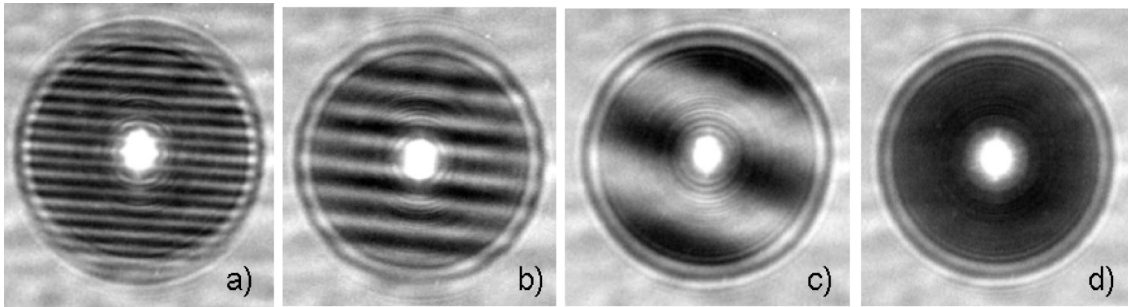


**Fig. 3** Experimental moiré patterns recorded at 12 keV for FZP 33 with 6  $\mu\text{m}$  (a), 3  $\mu\text{m}$  (b), 1  $\mu\text{m}$  (c) and 0  $\mu\text{m}$  (d) vertical lateral displacement. Images were taken at the position of the FZP focal plane (76 cm). Exposure time was 30 sec using CCD camera, therefore focus is completely overexposed. The aperture of the FZP is 200  $\mu\text{m}$ .

*moiré* pattern recorded at different distances from the stacked FZPs. The best pattern visibility and contrast was observed at distance corresponding FZP 1st order focusing. Figure 3 depicts *moiré* patterns recorded during vertical alignment with different displacements between zone plates. The fringe spacing is  $c = r_1^2/\Delta x$ , where  $r_1$  is the radius of the first zone. When zone plates are aligned with accuracy  $\Delta r_n$ , the spacing between fringes is equal lens aperture and for final lateral alignment intensity monitoring in the focus is required. A compact micro-mechanical motion system (piezo-based Y–Z stage) was used to execute such precise alignment with 50 nm step size (Fig. 4a).

For two zone plates to work effectively as one, the second element must be placed within the focal depth of the first one. Longitudinal alignment  $L$  must satisfy the condition  $L < 2\Delta r_n^2/\lambda$ . Figure 4b shows experimentally measured focus intensity versus the separation distance between two FZPs. It is clearly seen that separation up to 3 mm is acceptable ( $\sim 10\%$  intensity decrease) that is in good correspondence with requirements to longitudinal alignment. The focal depth at 12 keV is 3.2 mm.

The requirements for lateral and longitudinal alignments were studied theoretically [11]. Figure 5 shows intensity distribution along the optical distance versus the separation distance between FZPs (a) and the lateral displacement (b). Calculations were performed for 12 keV X-rays and FZP aperture was 250 micron and  $\Delta r_n = 100$  nm. For the FZP separation around 0.2 mm intensity drops down to 10%. Lateral misalignment up to 30 nm leads to 10% intensity decrease as well. When displacement is more than 150 nm the focus is split and each FZP focuses independently the zero order of the other FZP.

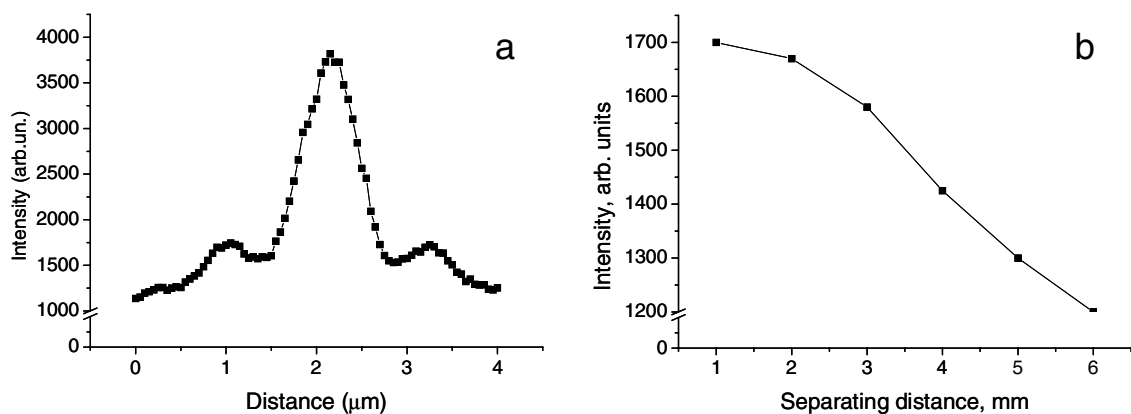


**Fig. 4** Intensity in the focal spot measured at 12 keV versus FZPs (33) lateral (a) and longitudinal displacement (b). Steps 50 nm for the lateral and 1 mm for longitudinal (FZPs separation) scans were used. A 10  $\mu\text{m}$  pinhole was placed in the focal plane of the FZP stack.

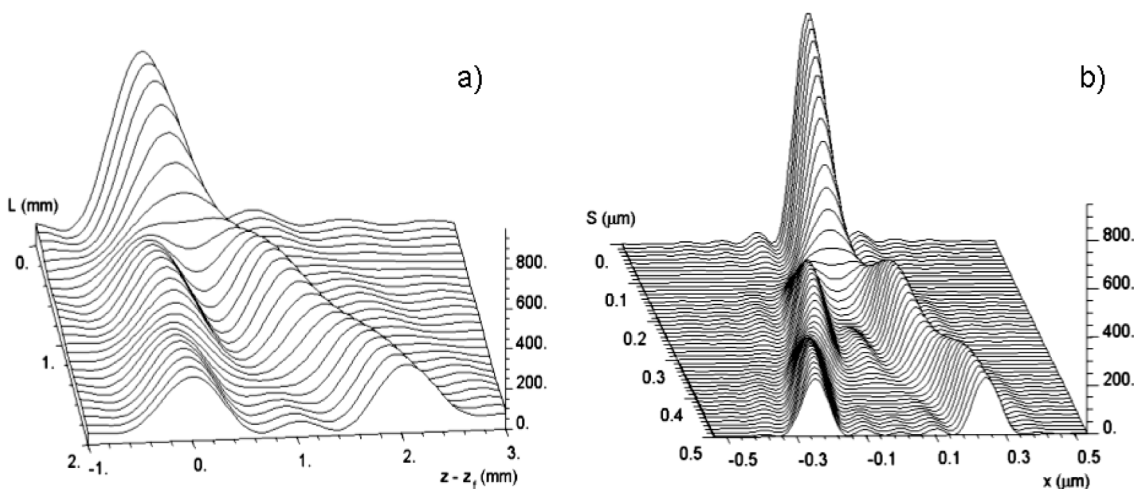


**Fig. 5** Calculated focus intensity distribution along the optical axis  $z$  at different distances  $L$  between FZPs (a) and intensity distribution across the focal spot for different lateral FZPs displacement (b).

To provide the desired stability and to use focusing elements at different beamlines, contrary to double zone plate holder approach [6, 7], we have bonded FZP chips. Slow solidification speed epoxy glue was used. We stacked two sets of FZPs: one is optimal for 15 keV and second for 50 keV X-rays. It was found that long-run gluing process introduces lateral misalignment in the order of 1 or 2  $\mu\text{m}$ . To compensate this displacement we have proposed the technique of angular alignment. Simple estimation shows that compensation tilt angle must be less than the ratio  $\Delta r_i/h$ , where  $h$  is FZP thickness. For example for 50 keV stack  $\Delta r_i/h = 0.013$  and lateral displacement up to 6  $\mu\text{m}$  for 500  $\mu\text{m}$  chip separation can be easily corrected with tilt. It was shown that lateral displacement in the order of 1  $\mu\text{m}$  can be compensated by sub-degree tilting, that is easily achievable with standard beamline equipment. Situation is more favorable for 15 keV stacking set, where displacement in the order of 25  $\mu\text{m}$  can be corrected. It should be emphasized that with angular alignment technique all 9 FZPs in the stack can be corrected and successfully used. Figure 6 shows X-ray images recorded with CCD camera at the position of the first focus without and with angular corrections.  $0.128^\circ$  angular rotation and  $0.065^\circ$  tilt compensations correspond to 2  $\mu\text{m}$  horizontal and less than 1  $\mu\text{m}$  vertical displacements.

The performance of the first set of stacked FZPs, which is optimal for 15 keV X-rays, has been tested at the MOTB of the BM05 beamline. High resolution X-ray CCD camera (pixel size 0.65  $\mu\text{m}$ ) was used to evaluate the size of the focal spot and FZP efficiency. FZP 33 with focal distance of 95 cm at 15 keV

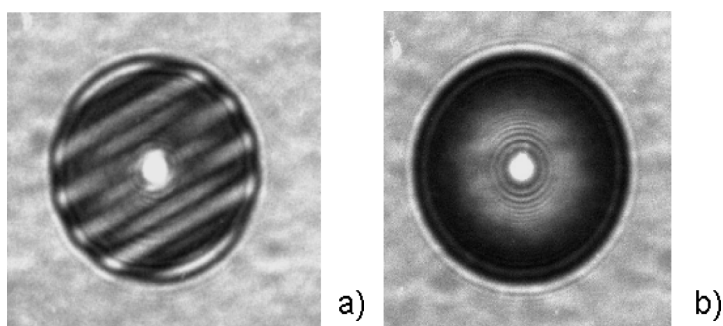


**Fig. 6** Experimental moiré patterns recorded at 12 keV FZP 33 at 76 cm; a) after gluing without angular correction, b) with  $0.128^\circ$  angular rotation and  $0.065^\circ$  angular tilt corrections. Exposure for both images was 15 sec.

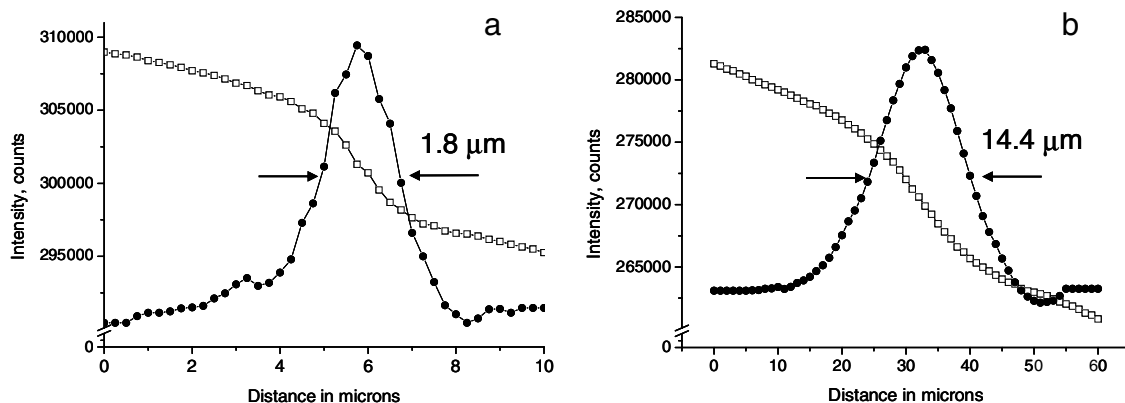


**Fig. 7** Vertical and horizontal scans. The high background is due to (i) the transparency of the knife, and (ii) the opening of the slit in front of the FZP, which is larger than its aperture; these do not affect the spot size measurements.

was chosen. Efficiency about 32% was measured. The gain in the efficiency compared with the single FZP is in the order of 2.5. The measured focal spot in the vertical direction was around  $2.5 \mu\text{m}$  that is a good agreement with the demagnification factor.

Optical properties of the second set of stacked FZPs were evaluated at the ID15 beamline at the ESRF. 50 keV X-rays were selected by using a horizontally deflecting Si crystal monochromator in Laue geometry. The set was placed at the distance 60 m from the source which is  $30 \mu\text{m}$  vertically and  $250 \mu\text{m}$  horizontally. A focal distance for FZP 33 was 3.3 m. The FZP alignment was done using a CCD camera with pixel size  $1.5 \mu\text{m}$ . But the lateral size of the microbeam was measured by scanning a  $35 \mu\text{m}$  thick Au knife-edge across the beam vertically and horizontally, recording the intensity by PIN diode detector. Focal spot of  $1.8 \mu\text{m}$  vertically and  $14 \mu\text{m}$  horizontally was measured (Fig. 7). The measured focal spot is in excellent agreement with calculations and underlines the good quality of the stacked system. Gain in the focal spot compared with the flat beam in slits the same size was measured as 450.

#### 4 Conclusion

Si-based FZP structures manufactured by means of microfabrication technology have been used for stacking. *Moiré* interference pattern was used for the on-line alignment. The formation of the *moiré* pattern was studied experimentally and theoretically during lateral and longitudinal alignments. Intensity monitoring was proposed for fine lateral adjustment within the first *moiré* fringe. Two sets of Si chips have been stacked and glued for focusing 15 and 50 keV X-rays. Technique of angular alignment to compensate a linear displacement was proposed. Intensity gain in the order of 2.5 was achieved compared to single FZP. The measured focal spot and efficiency are in excellent agreement with calculations and underlines the good quality of the stacked system. Our estimations show that stacking of three and more FZPs is straightforward with efficiency more than 20% above 100 keV. The proposed technique can be extended to nanofocusing FZP. To achieve the spatial resolution of 50 nm in the energy range 6–15 keV, a longitudinal proximity in the order of  $20 \mu\text{m}$  is required. Lateral alignment should be done within 15 nm, but with the proposed angular alignment technique lateral displacement in the order of 100 nm in the process of solidification can be compensated. For example the tilt angle of  $\sim 0.14^\circ$  is needed to compensate 50 nm lateral misalignments at 12 keV. From these simple estimations it is clear that stacking of nanofocusing FZPs is feasible.

**Acknowledgements** The authors wish to thank BM05 staff for the support during the experiment. One of the authors (M. Grigoriev) also acknowledges support from the INTAS postgraduate studentship program.

## References

- [1] H. Reichert, V. Honkimaki, A. Snigirev, S. Engemann, and H. Dosch, *Physica B* **336**, 46 (2003).
- [2] S. Engemann, H. Reichert, H. Dosch, J. Bilgram, V. Honimaki, and A. Snigirev, *Phys. Rev. Lett.* **92**, 205701 (2004).
- [3] D. Rudolph, B. Niemann, and G. Schmahl, *Proc. SPIE* **316**, 103–105 (1982).
- [4] K. Saitoh, K. Inagawa, K. Kohra, C. Hayashi, A. Iida, and N. Kato, *Rev. Sci. Instrum.* **60**, 1519–1523 (1989).
- [5] N. Kamijo, Y. Suzuki, H. Takamo, M. Yasumoto, A. Takeuchi, and M. Awaji, *Rev. Sci. Instrum.* **74**, 5101–5104 (2003).
- [6] S. D. Shastri, J. M. Maser, B. Lai, and J. Tys, *Opt. Commun.* **197**, 9–14 (2001).
- [7] J. Maser, B. Lai, W. Yun, S. D. Shastri, Z. Cai, W. Rodrigues, S. Xu, and E. Trackhtenberg, *Proc. SPIE* **4783**, 74–81 (2002).
- [8] I. Snigireva, A. Snigirev, G. Vaughan, M. Di Michele, V. Kohn, V. Yunkin, and M. Grigoriev, *AIP Conf. Proc.* **879**, 998–1002 (2007).
- [9] <http://www.esrf.fr/UsersAndScience/Experiments/Imaging/BM05/BeamlineGuide/EH2/MicroOpticsTest/>
- [10] A. G. Michette, *Optical systems for soft X-rays* (Plenum Press, New York, London, 1986).
- [11] V. G. Kohn, A. Snigirev, and I. Snigireva, *Crystallogr. Rep.* **51**, suppl. 1, S4–S11 (2006).